



The NuSTAR X-ray Spectrum of Hercules X-1: A Radiation-Dominated Radiative Shock



M.T. Wolff (Naval Research Laboratory), P.A. Becker (George Mason University), F. Fuerst (California Institute of Technology), P.B. Hemphill (University of California, San Diego), A. Gottlieb, D. Marcu-Cheatham, K. Pottschmidt (University of Maryland, Baltimore County), F.-W. Schwarm, J. Wilms (Dr. Karl-Remeis-Sternwarte and ECAP), K.S. Wood (Praxis)

Abstract

We report on new spectral modeling of an observation of the accreting X-ray pulsar Her X-1 by the Nuclear Spectroscopic Telescope Array (NuSTAR). We utilize a radiation-dominated radiative shock model that is an implementation of the analytic work of Becker & Wolff (2007) on Comptonized accretion flows onto magnetic neutron stars within the XSPEC analysis environment. We obtain a good fit to the Her X-1 spin-phase averaged 4 to 78 keV X-ray spectrum observed by NuSTAR during a main-on phase of the Her X-1 35-day accretion disk precession period. This model allows us to estimate the accretion rate, the Comptonizing temperature of the radiating plasma, the radius of the magnetic polar cap, and the average scattering opacity parameters in the accretion column. This is in contrast to previous spectral models that characterized the shape of the X-ray spectrum but could not determine the physical parameters of the accretion flow. We describe the details of our spectral fitting model and we discuss the interpretation of the resulting accretion flow physical parameters.

This research is supported by the NASA Astrophysical Data Analysis Program.

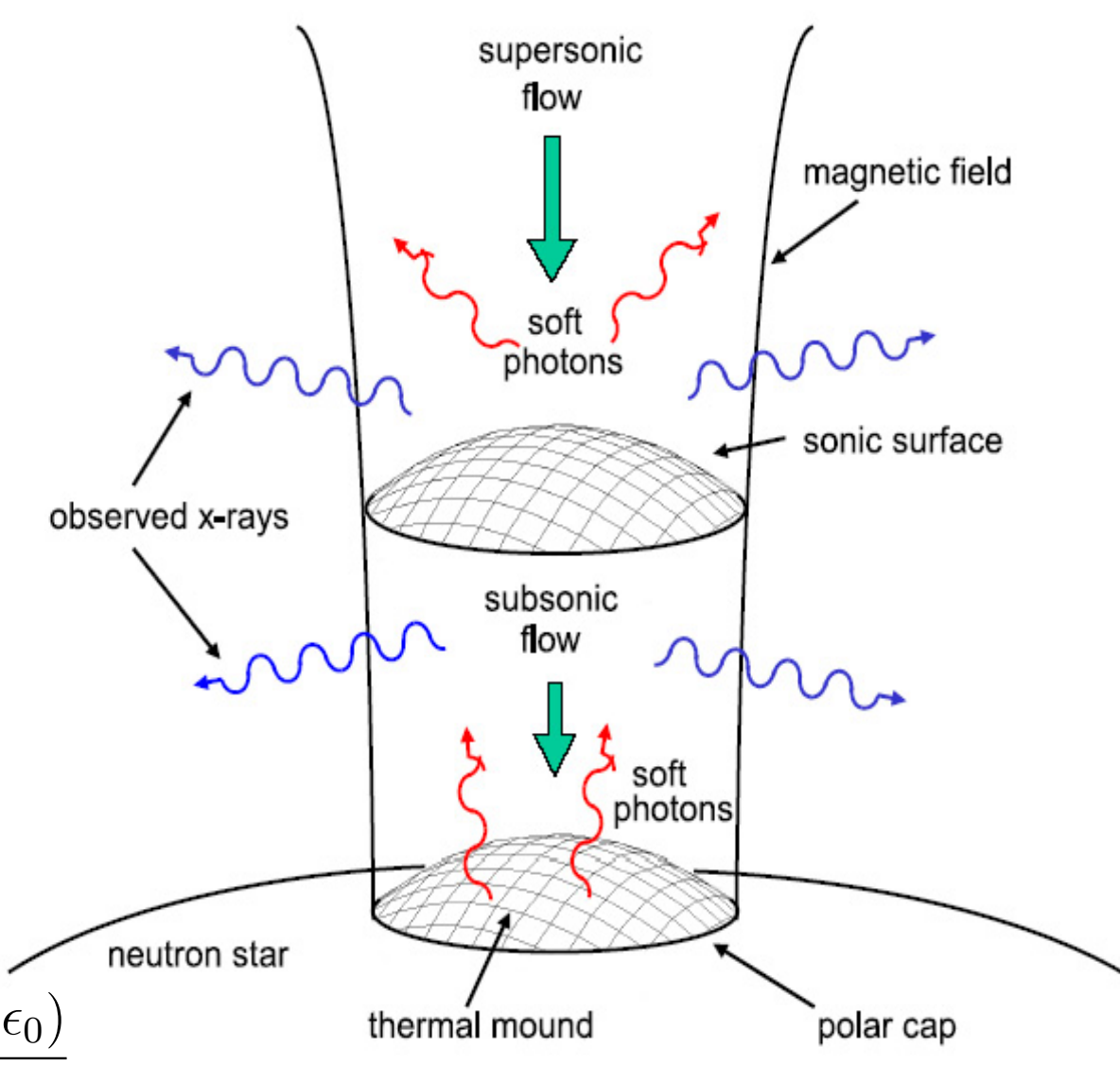
Developing A New Modeling Tool

We ask: Can the energy and shape of the observed cyclotron resonant scattering features (CSRFs) be uniquely tied to the production of the X-ray continuum via a single, self-consistent physical model? We develop spectral analysis tools to answer this question and utilize the HEASoft/XSPEC analysis environment to analyze data from a number of high signal-to-noise accreting X-ray pulsars to test the model. (See schematic below)

Seed photons that will be Comptonized are created in column plasma by Bremsstrahlung and cyclotron emission, with blackbody photons emitted from the thermal mound surface near the base of the column.

We model the photon distribution function Green's function f_G in the radiation-dominated plasma utilizing the transport equation including bulk and thermal Comptonization (see Becker & Wolff 2007):

$$v \frac{\partial f_G}{\partial z} = \frac{dv}{dz} \frac{\partial f_G}{\partial v} + \frac{\partial}{\partial z} \left(\frac{c}{2n_e \sigma_T} \frac{\partial f_G}{\partial z} \right) - \frac{f_G}{t_{esc}} + \frac{n_e \sigma_T c}{m_e c^2} \frac{1}{v^2} \left[\epsilon^A (f_G + kT_e \frac{\partial f_G}{\partial \epsilon}) \right] + \frac{\dot{N}_0 \delta(z - z_0) \delta(\epsilon - \epsilon_0)}{\pi r_0^2 \epsilon_0^2}$$



We compute radiation spectrum distribution $f_G(z, \epsilon)$, by convolving f_G with a source photon distribution $\dot{N}_0 \delta(z - z_0) \delta(\epsilon - \epsilon_0)$ Bremsstrahlung + Cyclotron + Blackbody; see also Becker & Wolff (2005)).

The evaluation of the X-ray spectrum centers on the series expressions below. These three series represents the contribution to the column-integrated spectrum from Compton scattering energization of seed photons from the radiative processes bremsstrahlung, cyclotron emission, and blackbody emission from a thermal mound. Being optimized for rapid evaluation, they enable rapid exploration of a large parameter space. For details see Wolff *et al.*, 2016, ApJ, (submitted).

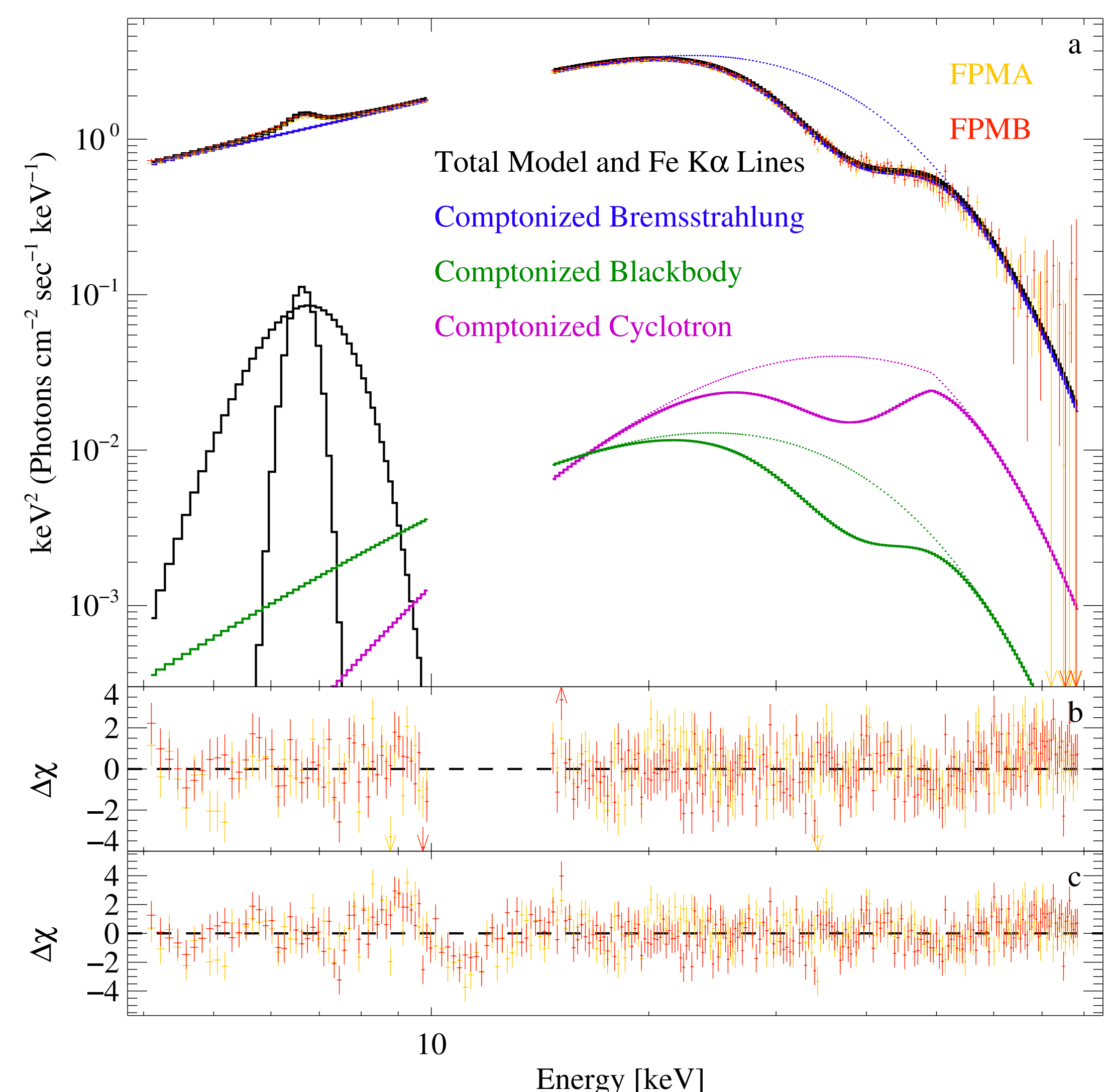
$$\Phi_{\epsilon}^{ff}(\epsilon) = \frac{2.80 \times 10^{-12} \dot{M} \xi^2 \sqrt{\alpha^3} w \epsilon^{\kappa-2} e^{-\epsilon/(2kT_e)} \sum_{n=0}^{\infty} \frac{\Gamma(\mu_n - \kappa + 1/2) n!}{\Gamma(1 + 2\mu_n) \Gamma(n + 1/2)} X_n A_n \times \int_{\chi_{abs}}^{\infty} \left(\frac{\epsilon_0}{kT_e} \right)^{-1-\kappa} \exp\left(-\frac{\epsilon_0}{2kT_e}\right) M_{\kappa, \mu_n} \left(\min\left[\frac{\epsilon}{kT_e}, \frac{\epsilon_0}{kT_e}\right] \right) W_{\kappa, \mu_n} \left(\max\left[\frac{\epsilon}{kT_e}, \frac{\epsilon_0}{kT_e}\right] \right) d\epsilon_0$$

$$\Phi_{\epsilon}^{bb}(\epsilon) = \frac{6\pi^2 r_0^2 \delta \xi^2 kT_e \sqrt{2\alpha^3} w \exp\left(-\frac{3\alpha\tau_{th}^2}{2}\right) \epsilon^{\kappa-2} \exp\left(-\frac{\epsilon}{2kT_e}\right)}{c^2 h^3} \times \sum_{n=0}^{\infty} \frac{\Gamma(\mu_n - \kappa + 1/2) n! X_n g_n(\tau_{th})}{\Gamma(1 + 2\mu_n) \Gamma(n + 1/2)} \left[W_{\kappa, \mu_n} \left(\frac{\epsilon}{kT_e} \right) \int_0^{\epsilon} M_{\kappa, \mu_n} \left(\frac{\epsilon_0}{kT_e} \right) \frac{\epsilon_0^{2-\kappa} \exp\left(-\frac{\epsilon_0}{2kT_e}\right)}{\exp\left(\frac{\epsilon_0}{kT_e}\right) - 1} d\epsilon_0 + M_{\kappa, \mu_n} \left(\frac{\epsilon}{kT_e} \right) \int_{\epsilon}^{\infty} W_{\kappa, \mu_n} \left(\frac{\epsilon_0}{kT_e} \right) \frac{\epsilon_0^{2-\kappa} \exp\left(-\frac{\epsilon_0}{2kT_e}\right)}{\exp\left(\frac{\epsilon_0}{kT_e}\right) - 1} d\epsilon_0 \right]$$

$$\Phi_{\epsilon}^{cyc}(\epsilon) = \frac{3.43 \times 10^{-16} \dot{M} H(\epsilon_c/(kT_e)) \xi^2 \sqrt{\alpha^3} w \epsilon^{\kappa-2} \sum_{n=0}^{\infty} \frac{\Gamma(\mu_n - \kappa + 1/2) n!}{\Gamma(1 + 2\mu_n) \Gamma(n + 1/2)} X_n A_n \exp[\epsilon_c/(kT_e)]}{\bar{\sigma} \epsilon_c^{\kappa+3/2} \exp[\epsilon_c/(kT_e)]} \times M_{\kappa, \mu_n} \left(\min\left[\frac{\epsilon}{kT_e}, \frac{\epsilon_c}{kT_e}\right] \right) W_{\kappa, \mu_n} \left(\max\left[\frac{\epsilon}{kT_e}, \frac{\epsilon_c}{kT_e}\right] \right)$$

$$F_{\epsilon}(\epsilon) \equiv \frac{[\Phi_{\epsilon}^{cyc}(\epsilon) + \Phi_{\epsilon}^{bb}(\epsilon) + \Phi_{\epsilon}^{ff}(\epsilon)] A_c(\epsilon)}{4\pi D^2}$$

Test Modeling Tool: NuSTAR Her X-1 Observation



Application to Hercules X-1 data from NuSTAR. Curves show Comptonized components and their sum, compared with data from FPMA, FPMB. Residuals are at bottom. From Wolff *et al.*, 2016, ApJ, (submitted).

Broader Utilization of New Tool

Our goal is to utilize the spectral modeling tool with pulsar data in X-ray archives. The Table below shows broader program currently in progress.

Source Name	X-ray Luminosity [ergs/s]	Magnetic Field [G]	Pulse Period [s]	System Type
4U 0115+634	$\leq 2 \times 10^{38}$	$\sim 1.2 \times 10^{12}$	3.6	Transient
GX 304+1	$\leq 2 \times 10^{37}$	$\sim 4.7 \times 10^{12}$	272	Transient
V 0332+53	$\leq 5 \times 10^{38}$	$\sim 2.7 \times 10^{12}$	4.4	Transient
A 0535+26	$\leq 1 \times 10^{37}$	$\sim 4.0 \times 10^{12}$	105	Transient
Vela X-1	$\sim 6.0 \times 10^{36}$	$\sim 2.7 \times 10^{12}$	283	Persistent + Eclipsing
Her X-1	$\sim 2.5 \times 10^{37}$	$\sim 4.4 \times 10^{12}$	1.24	Persistent + Eclipsing
Cen X-3	$\sim 1.0 \times 10^{38}$	$\sim 3.3 \times 10^{12}$	4.82	Persistent + Eclipsing
LMC X-4	$\sim 4.0 \times 10^{38}$	$> 10^{13}$ (?)	13.5	Transient
SMC X-1	$\sim 8.0 \times 10^{38}$	Not known	0.716	Persistent + Eclipsing

Further spectral fitting with this new implementation of the Becker & Wolff model can be found in HEAD Poster 120.09 (Amy Gottlieb *et al.*) and Diana-Cheatham talk in HEAD Special Session 201 on GX 304-1, XTE J1946-274, and LMC X-4.

References:

Wolff *et al.*, 2016, ApJ, (submitted)
Becker & Wolff 2005, ApJ, 630, 465.
Becker & Wolff 2007, ApJ, 654, 435.